

Improvement of the accuracy of Hogg and Fuerstenau's model in predicting the power draw of ball mills based on determining the grinding media's dynamic voidage

Mohammad Hasan Golpayegani, Bahram Rezai

Mining engineering faculty, Amirkabir University of Technology, Tehran, Iran

Corresponding author: Rezai@aut.ac.ir (Bahram Rezai)

Abstract: In the development of tumbling mills' power models, the voidage of grinding media is assumed to be static and equal to 40%. While the grinding media's voidage is dynamic; and hence is varied by changing the operating parameters. In this paper, to improve the Hogg and Fuerstenau model's accuracy in predicting the ball mills' power draw, the grinding media's static and dynamic voidage was studied for Bond's proposed ball size distributions (BSD) for the ball mills' first filling. To this end, by scaling down balls to one-tenth of actual size, developing a novel method to measure the dynamic voidage, and employing the three-level factorial method, a separate empirical model was developed for determining the dynamic voidage of each Bond's BSD with respect to mill's fractional filling and rotating speed. Moreover, using the multiple regression method, a general empirical model was derived to determine the dynamic voidage of each supposed BSD based on calculating the mean absolute deviation of balls diameter (MAD). Results indicated that grinding media's dynamic voidage increases with an increase in rotating speed and a decrease in fractional filling and balls diameter's MAD. The maximum and minimum static and dynamic voidage occurred for the seventh and first Bond's BSDs. By employing an industrial database and analyzing the mean absolute percentage error (MAPE) of predicted ball mills' power draw, it was found that the Hogg and Fuerstenau model's accuracy enhances by calculating the load's bulk density based on the grinding media's dynamic voidage.

Keywords: voidage, grinding media, ball mill, Hogg and Fuerstenau's model, power draw

1. Introduction

Tumbling mills can be considered the heart of the metal production processes because all minerals used as feed for mineral and metallurgical processes must be first ground (Wills and Finch, 2015). Literature indicates that grinding accounts for approximately 40% of the mining industry's total energy consumption and more than 50 % of mineral processing plants' operating costs (Corneille, 1987; U.S. DOE, 2007). Besides, decreasing the ores' average grade in most mines worldwide causes strikingly enhances the cost of energy per unit of produced metal (Valery and Jankovic, 2002). Since the largest mills' electricity consumption is about 20-30 MW, even a tenth percent reduction in energy consumption provides tremendous annual energy savings for mineral processing plants (Drzymala, 2007; Goralczyk et al., 2020). To increase mills' efficiency, equipment designers have attempted to improve all ball mill components, including bearings, gear drivers, lubrication systems, and the electric motor. However, one of the main significant problems leading to the low energy efficiency of mills is that about 30% of grinding bodies remain in a dead zone and are not involved in the dynamic processes (Goralczyk et al., 2020; Golpayegani and Rezai, 2022). Accordingly, new technologies such as the Vertimill (Metso) and the horizontal Isamill (Glencore Technology) have been introduced, which use gravitation forces or rotating discs to maximize the live area of the mill (Mogroup, 2022; Glencoretechnology; 2022). In addition, to prevent the transmission of grinding media in the dead zone, researchers have focused on using electromagnets embedded in the mill shells (Wołosiewicz-Głab et al., 2016; Wołosiewicz-Głab et

al., 2017; Krawczykowski et al., 2018; Foszcz et al., 2019). However, traditionally designed ball mills are still the main part of mineral processing plants in the world (Golpayegani and Rezai, 2022).

Based on those mentioned above, optimizing and reducing power consumption are essential factors in mineral processing plants' design and control of the operational parameters to reduce grinding costs. To this end, developing a capable model to accurately predict the mills' power draw took the attention of researchers, tumbling mill manufacturers, and process engineers. Literature indicates that the charge shape's description inside the tumbling mills and the analysis approach of milling operation are vital parameters in modeling the tumbling mills' power draw. Accordingly, provided models can be classified under two generalized categories: empirical and fundamental. Moreover, the fundamental models can be classified under four subsets: energy balance, friction approach, torque-arm, and discrete element method (DEM) (Morrell, 2019; Tavares, 2017; Golpayegani and Rezai, 2022). Davis (1919) established the first relationship between charge motion in a ball mill and its power draw using White's description of the charge motion (White, 1905). Other charge shape descriptions were provided by Hogg and Fuerstenau (1972), Liddell and Moys (1988), Moys (1993), and Morrell (1993). Besides, in the last two decades, the DEM has contributed to understanding the mills' charge shape and its impact on the tumbling mills' power draw. (Mishra and Rajamani, 1992; Djordjevic, 2003; Erdem et al., 2004; Kiangi et al., 2013; Zhang et al., 2014; Govender et al., 2015; Panjipour and Barani, 2014; Govender et al., 2018; Gutiérrez et al., 2019; Cleary and Owen 2019; Hlosta et al. 2020; Amannejad and Barani 2020).

Among empirical models, the Bond model and Morrell E-model have been employed as valid models for predicting the power draw of ball mills and AG/SAG mills in industry, respectively. Moreover, the Morrell C-model and Hogg and Fuerstenau's model are reported as the most accurate fundamental models for predicting the power draw of tumbling mills, respectively (Morrell, 1993; Rajamani et al., 2019). In all developed models, the mill charge's bulk density is one of the significant, influential variables estimated based on the grinding media density, the ore density, and the grinding media voidage (Morrell 2016; Hilden et al. 2021). The grinding media voidage has been assumed to be 40 % in all developed models, while documented investigations on how the voidage is determined are not accessible. Based on the published studies on the particle bed's voidage, the value of 40 % has been obtained for a bed of mono-sized spherical particles under vibration while grinding media inside the industrial mills is a combination of multi-sized particles (Yang, 2003). Moreover, the grinding media voidage has been assumed constant during operation and equal to the balls' static voidage when a mill is not running. While mill load is dynamic, its voidage may be changed by any change in operating parameters such as rotating speed, fractional mill filling, and size distribution of grinding media. Accordingly, Latchireddi (2002) attempted to prepare an Eq. to predict the value of grinding media's dynamic voidage. However, he used mono-sized balls, whereas, in industrial mills, there is a distribution of ball sizes called the equilibrium distribution or seasoned charge distribution. Hence, it is necessary to develop a relationship that can estimate the grinding media voidage in various operating conditions by considering a more realistic ball size distribution (BSD).

The ball size distribution for the first filling of ball mills is typically selected based on Table 1s proposed by Bond (1958). Of course, balls' shape and size distribution under various factors, including impact, erosion, corrosion, and crushing, change over time. Since equipment power draw is repeatedly checked and analyzed during the mineral processing plants' commissioning, the voidage of each BSD proposed by Bond must be considered in preparing Eqs. for determining the grinding media voidage.

Design of Experiments (DOE) is a useful method allowing researchers to plan the experiments and analyze the cause-and-effect between operating parameters in a process. The DOE is extensively used in numerous investigation fields because it decreases the number of experiments that need to be conducted (Montgomery, 2005). Several experimental designs have been recognized as practical techniques so far. The RSM is an efficient tool of DOE, which is widely applied to provide a mathematical relationship between a dependent parameter (output response) and independent variables (inputs). Furthermore, utilizing RSM contributes to accurately analyzing the effect of variable parameters and their interaction on the output response (Soleymani Yazdi and Khorram, 2010).

In this work, the grinding media's static and dynamic voidage inside the ball mills were studied to improve the accuracy of Hogg and Fuerstenau's model in predicting the ball mills' power draw. The three-level factorial design, one of the most efficient and foremost essential RSM tools, was employed

to model the dynamic voidage of grinding media. The fractional mill filling and mill rotating speed were considered as the variable input parameters. Based on this, a separate model was developed for each ball size distribution proposed by Bond, which can be used to calculate the apparent charge density in ball mill settings and typical ball mill operating conditions. In addition, a general Eq. was developed by the multiple regression method to predict the dynamic discharge of different BSDs based on the calculation of the mean absolute deviation of balls diameter. Finally, the dynamic voidage prediction models' performances in increasing the accuracy of Hogg and Fuerstenau's model were examined using a ball mills' industrial database and assessing the models' prediction results' mean absolute percentage error (MAPE).

2. Hogg and Fuerstenau's model

A description of charge motion must first be provided to develop a fundamental power Eq. for the tumbling mills. Davis (1919) was the first person to establish a relationship between a ball mill's charge motion and its power draw using the energy balance approach. Davis' description is similar to the earliest reports provided by White (1905). In this description, the particles move in a locked manner in a circular path until a point where the gravitational and centrifugal forces balance. At this point, particles experience a parabolic free fall until they impact the bed, and afterward, they return to the circular path again. The locus of free fall points occurs on a circle's circumference with a $\frac{g}{2\omega^2}$ radius, called "Davis Circle" (see Fig. 1a).

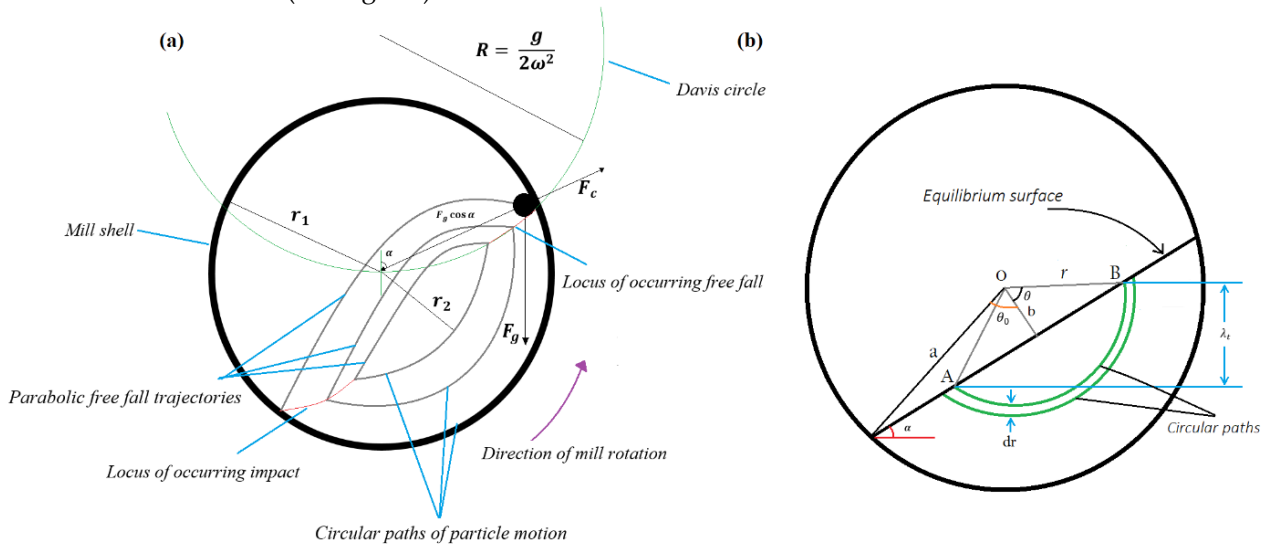


Fig. 1. Schematic of the descriptions of charge motion. (a) Davis' description (Davis 1919), (b) Hogg and Fuerstenau's description (Hogg and Fuerstenau 1972)

Hogg and Fuerstenau (1972) remarked that Davis' description has two following shortcomings: (1) the quantity of material (ball filling) has been ignored, and (2) The circular paths shown in Fig. 1a cannot cross each other at any moment, which it is an unrealistic assumption. Hence, they provided a new description in which it is assumed that the mill charge includes two distinct parts: a 'static' part moved with the mill shell and a 'shear' region in which particles flow down on the charge's surface (see Fig. 1b). In this description, the mill motor should supply energy to raise the balls in each circular path through the static part from the toe to the shoulder. Since the milling system is in the dynamic equilibrium condition, an assumed particle should have the same energy when it is at the same location in the mill. Hence, the particles' potential energy ($mg\lambda_t$) in the bed's static part is completely lost in the shear zone. Based on these assumptions, the following simple power Eq. was derived using the energy balance approach:

$$P = \frac{2}{3} \rho_{\text{bulk}} g^2 L N_c \left(\frac{D}{2}\right)^{2.5} \sin^3 \theta_0 \sin \alpha \quad (1)$$

where P is the power draw (kW), D is the mill effective diameter (ft.), L is the mill effective length (ft.), ρ_{bulk} is the mill charge's bulk density (tonnes/m³), α is the charge's angle of repose (typically in the

range of 30° to 35°), N_c is the fractional speed, and θ_0 is the filling angle associated with the fractional mill filling (in radians). Moreover, Hogg and Fuerstenau (1972) provided the following Eq. to calculate the mill charge's bulk density (ρ_{ap}):

$$\rho_{ap} = [(1-\varphi) \rho_b J_b + \rho_p J_p \varphi J_b + \rho_p (J-J_b)]/J \quad (2)$$

where φ is the grinding media voidage, ρ_b is the steel balls density (tonnes/ m^3), J_b is the fractional mill filling by steel balls, ρ_p is the slurry density (tonnes/ m^3), J is the total fractional filling, J_p is the interstitial slurry filling, corresponding to the fraction of the available interstitial voids (in between the ball charge) actually occupied by the slurry. It must be mentioned that Eq. 1 gives the power of mill pinion, and hence to estimate the gross power draw, the motor and gearbox energy losses must be considered. This loss is reported at 4% and 3% for the motor and gearbox (Morrell 1993).

Literature indicates that Hogg and Fuerstenau's model can acceptably predict the mills' power draw (Rajamani et al., 2019; Doll, 2016). For this reason, the Moly-Cop tools, which have been provided to assess grinding media performance at a full industrial scale, use Hogg and Fuerstenau's model to estimate the industrial mills' net power draw (Molycop, 2021).

According to Eq. 2, the grinding media voidage is a vital parameter in estimating the charge bulk density. As mentioned above, all power Eqs. assumed the voidage of the active charge during operation to be equal to the static voidage, which is usually supposed to be equivalent to a constant value of 40%. While the mill charge has a dynamic state during milling operation, and its voidage is changed with changing operating conditions such as rotating speed, fractional mill filling, and balls' size distribution. Hence this paper has attempted to develop an empirical Eq. to determine the grinding media's dynamic voidage in various operating conditions by considering the more realistic ball size distribution.

3. Materials and methods

3.1. Materials

Different ball size distributions proposed by Bond for ball mills' first filling in commissioning stage, obtained from scale down of the balls' size to one-tenth of the presented sizes in Table 1s, were used as grinding media (Fig. 2a). A laboratory-scale glass-fronted ball mill with a length and diameter of 14 cm was used (Fig. 2b). 4 square cross-section lifters with a side length of 9 mm were installed in the mill shell, as shown in Fig. 2c. The rotating speed was adjusted with a variable-frequency drive (VFD). It should be noted that to remove the wall effect on the value of voidage, the diameter of the mill should be at least ten times the diameter of the largest balls, which was 11.5 mm in this study (Benyahia and O'Neill, 2005). Furthermore, the Design-Expert software was employed for designing experiments, developing models, and analyzing graphs. Besides, the Minitab software was used to develop a multiple regression model.

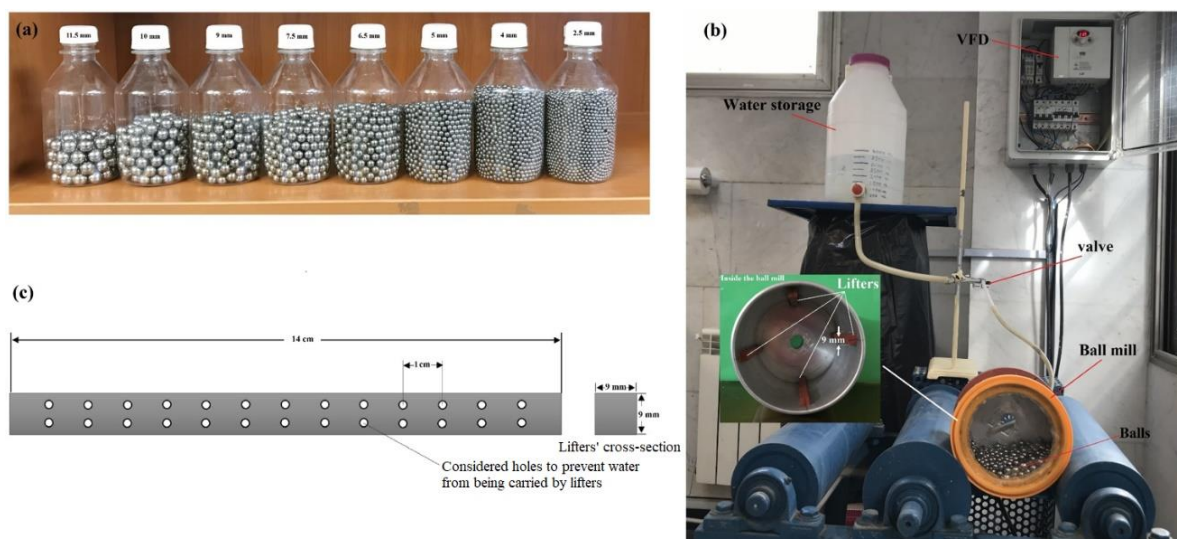


Fig. 2. Equipment employed. (a) Employed balls to prepare Bond's proposed ball size distributions. (b) A schematic of all equipment and instruments used. (c) A simple general arrangement of lifters

3.2. Experimental procedure

First, based on the ball size distribution and fractional mill filling, the required weight of each ball size fraction was weighed and then charged to the ball mill. Then the mill's rotating speed was adjusted using VFD. Once the shape of the load reached steady-state, the water pipeline valve was opened. Water was added until a circular segment with a measurable area appeared on the mill's glass-fronted surface (Fig. 3). Then, the sagitta (height) of the circular segment (h) was measured by an adjustable T-Square ruler (Fig. 3). Finally, water was discharged and weighed. To prevent water from being carried by the lifters, 26 holes were made in each lifter's body with a diameter of 2 mm, which was less than the smallest balls' diameter (see Fig. 2c).

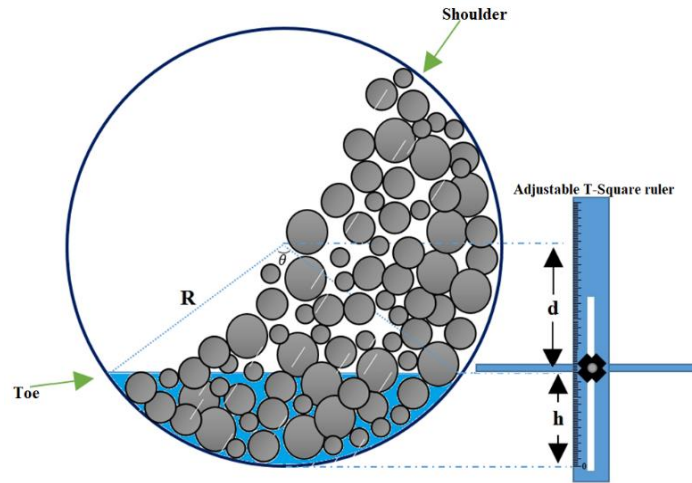


Fig. 3. A schematic of the shape of materials inside a mill during operation

For each experiment, the volume of the cylindrical segment of the ball mill occupied by a combination of water and balls was given through the following Eqs. (Harris and Stocker, 1998):

$$V=AL \quad (2)$$

$$A=\frac{R^2}{2}(\theta-\sin\theta) \quad (3)$$

$$\theta=2\arccos\left(\frac{R-h}{R}\right) \quad (4)$$

where V is the cylindrical segment volume (m^3), A is the circular segment area (m^2), L is the mill inside length (m), R is the mill inside radius (m), and θ the central angle (radians).

By calculating the cylindrical segment volume occupied by water and balls (V) and water volume (V_w), which is equal to its weight, the grinding media's dynamic voidage (ϕ) was obtained as follow:

$$\phi = \frac{V_w}{V} \quad (6)$$

For more precise analyses of the effect of grinding media size distribution on voidage value, we also measured the static voidage of all BSDs presented in Table 1s.

3.3. Design of experiments

The surface response methodology (RSM), a combination of statistical and mathematical techniques, has been widely employed to model and analyze the processes in which a dependent parameter is affected by various independent parameters simultaneously. Different RSM design types comprise factorial design, central composite design (CCD), D-optimal design, and Box-Behnken design (Montgomery, 2005; Golpayegani and Abdollahzadeh, 2017).

In this work, the three-level factorial design, one of the most efficient methods among other response surface designs, was employed to design experiments and model the grinding media voidage by considering the fractional mill filling and the mill rotating speed as independent parameters. The input includes three levels of two independent parameters: upper and lower axes and an average value. Table 1 shows the coded and considered actual levels of the fractional mill filling and the mill rotating speed. The designed experiments (91 experiments by considering 13 for each BSD) are shown in Table 2.

Table 1. Design level in the coded and actual level

Parameters	Symbol	Units	Coded and actual levels		
			-1	0	1
Fractional mill filling	J	%	15	30	45
Fraction of mill critical speed	Cs	%	40	65	90

Table 2. Designed experiments by Three-level factorial design and obtained results

Run No.	J (%)	Q (%)	Grinding media voidage (%)													
			BSD ₁		BSD ₂		BSD ₃		BSD ₄		BSD ₅		BSD ₆		BSD ₇	
			Experimental	Predicted	Experimental	Predicted	Experimental	Predicted	Experimental	Predicted	Experimental	Predicted	Experimental	Predicted	Experimental	Predicted
1	30	65	36.43	36.43	37.43	37.44	38.73	38.62	39.61	39.54	40.30	40.34	41.26	41.42	43.23	43.22
2	45	40	35.61	35.60	36.14	36.08	37.21	37.13	38.08	38.00	38.72	38.65	39.6	39.49	41.22	41.08
3	30	90	37.24	37.21	38.62	38.63	39.97	39.88	40.86	40.77	41.70	41.62	43.19	43.04	45.08	44.96
4	30	65	36.40	36.43	37.46	37.44	38.69	38.62	39.44	39.54	40.39	40.34	41.48	41.42	43.35	43.22
5	45	65	35.98	35.94	36.64	36.7	37.80	37.81	38.69	38.76	39.53	39.56	40.54	40.56	42.14	42.23
6	30	65	36.40	36.43	37.54	37.44	38.55	38.62	39.59	39.54	40.30	40.34	41.5	41.42	43.22	43.22
7	30	40	35.68	35.79	36.26	36.41	37.33	37.54	38.27	38.38	38.85	38.99	39.68	39.91	41.34	41.57
8	45	90	36.36	36.42	37.48	37.48	38.60	38.67	39.56	39.57	40.37	40.40	41.66	41.75	43.42	43.46
9	30	65	36.50	36.43	37.50	37.44	38.61	38.62	39.60	39.54	40.40	40.34	41.47	41.42	43.14	43.22
10	15	65	39.69	39.81	40.69	40.79	41.92	42.03	43.22	43.17	43.89	43.91	44.79	44.85	46.79	46.82
11	30	65	36.51	36.43	37.40	37.44	38.64	38.62	39.50	39.54	40.36	40.34	41.48	41.42	43.26	43.22
12	15	40	38.96	38.87	39.43	39.35	40.68	40.54	41.63	41.60	42.19	42.12	43.03	42.9	44.77	44.67
13	15	90	40.92	40.89	42.40	42.38	43.67	43.69	44.73	44.81	45.59	45.64	46.84	46.9	48.98	49.06

4. Results and discussion

4.1. Statistical analysis

A three-level factorial response surface design with two independent variables comprised of fractional filling and mill rotating speed was used to examine the effects of variables on the dependent variable (voidage of grinding media). The obtained values of grinding media voidage (reported in Table 2) were inserted into DOE. Then, the analysis of variance (ANOVA) as a beneficial statistical tool was used to analyze data and generate a mathematical model for each BSD shown in Table 1s.

Table 3 reports the Linear, cross-product contribution (2FI), quadratic, and cubic models generated in the Design expert software's response for different ball size distributions (BSD₁ to BSD₇). As can be seen, the quadratic model with the following general Eq. was suggested to estimate the dynamic voidage of all BSDs based on the models' statistics of response (Montgomery, 2005):

$$Y=A+BX_1+CX_2+DX_1X_2+EX_1^2+FX_2^2 \quad (7)$$

where A is the intercept, B to F are the estimated coefficient obtained from the experimental value of Y, and X₁ and X₂ are the independent variables.

The ANOVA, which considers the variances' ratio according to the Fisher method, was used to assess the significance of generated models and variable effects on the response. In the Fisher method procedure, the significance of a model or a parameter effect is dependent on the F and P values so that the lower level of the p-value (P < 0.05) and upper level of the F-value prove the significance of a parameter at the confidence interval of 95 % (Montgomery, D.C., 2005). The F and P values of models and the significant parameters are reported in Table 2s. From Table 2s, it can be concluded that the fractional mill filling (J_t), the rotating speed (C_s), their interaction (J_t * C_s), and the quadratic term of

fractional mill filling (J_t^2) are significant factors in all models. Hence, Eqs. 8 to 14 were obtained to estimate the grinding media voidage of BSD₁ to BSD₇, respectively:

$$\phi_1 = +43.12158 - 0.462313J_t + 0.038590C_s - 0.000804J_t C_s + 0.006424J_t^2 \quad (8)$$

$$\phi_2 = +42.28959 - 0.414306J_t + 0.060327C_s - 0.001087J_t C_s + 0.005812J_t^2 \quad (9)$$

$$\phi_3 = +43.51516 - 0.417540J_t + 0.060085C_s - 0.001070J_t C_s + 0.005776J_t^2 \quad (10)$$

$$\phi_4 = +44.61249 - 0.455356J_t + 0.074383C_s - 0.001087J_t C_s + 0.006311J_t^2 \quad (11)$$

$$\phi_5 = +44.34998 - 0.441269J_t + 0.094564C_s - 0.001171J_t C_s + 0.006204J_t^2 \quad (12)$$

$$\phi_6 = +44.88569 - 0.409801J_t + 0.085930C_s - 0.001161J_t C_s + 0.005708J_t^2 \quad (13)$$

$$\phi_7 = +46.32825 - 0.413476J_t + 0.098013C_s - 0.001340J_t C_s + 0.005793J_t^2 \quad (14)$$

In these models, all variables are in actual values. By employing these Eqs., the grinding media voidage and subsequently the bulk density of ball mills' charge can be predicted in the ball mills' commissioning stage. Besides, considering the changes in the grinding media's shape and size under the various factors, including impact, attrition, corrosion, and chipping, it can be assumed that the actual ball size distribution inside ball mills is approximately close to BSD₁. Hence, by replacing the response of Eq. 8 into Eq. 2 as the value of grinding media voidage (ϕ_t), the mill charge's bulk density is obtained for a given operational condition of ball mills.

Table 3. The models' summary statistics of response

Response		Model	Lack of Fit p-value	Adjusted R ²	Predicted R ²	Significance
ϕ_1	Dynamic voidage of BSD ₁	Linear	< 0.0001	0.7299	0.5394	-
		2FI	< 0.0001	0.7146	0.0809	-
		quadratic	0.0725	0.9972	0.9871	Suggested
		cubic	0.1535	0.9986	0.9671	Aliased
ϕ_2	Dynamic voidage of BSD ₂	Linear	< 0.0001	0.7989	0.6438	-
		2FI	< 0.0001	0.7993	0.3251	-
		quadratic	0.0578	0.9972	0.9891	Suggested
		cubic	0.0253	0.9972	0.8965	Aliased
ϕ_3	Dynamic voidage of BSD ₃	Linear	< 0.0001	0.8107	0.6668	-
		2FI	< 0.0001	0.8104	0.3691	-
		quadratic	0.0515	0.9951	0.9768	Suggested
		cubic	0.1128	0.9976	0.9411	Aliased
ϕ_4	Dynamic voidage of BSD ₄	Linear	< 0.0001	0.8050	0.6662	-
		2FI	< 0.0001	0.8030	0.3917	-
		quadratic	0.2319	0.9976	0.9906	Suggested
		cubic	0.8079	0.9987	0.9982	Aliased
ϕ_5	Dynamic voidage of BSD ₅	Linear	< 0.0001	0.8165	0.6823	-
		2FI	< 0.0001	0.8186	0.4459	-
		quadratic	0.0550	0.9981	0.9909	Suggested
		cubic	0.2079	0.9993	0.9871	Aliased
ϕ_6	Dynamic voidage of BSD ₆	Linear	0.0002	0.8412	0.7208	-
		2FI	0.0002	0.8443	0.4980	-
		quadratic	0.1053	0.9943	0.9741	Suggested
		cubic	0.3435	0.9974	0.9712	Aliased
ϕ_7	Dynamic voidage of BSD ₇	Linear	< 0.0001	0.8533	0.7378	-
		2FI	< 0.0001	0.8612	0.5492	-
		quadratic	0.0526	0.9958	0.9800	Suggested
		cubic	0.1563	0.9982	0.9623	Aliased

Since an inadequate model could lead to inaccurate results, a model's validation based on the model outputs' precision is essential for data analysis. Hence, the adequate precision ratio's value which indicates the accuracy of a model's outputs is a critical factor. For a model to be valid, this ratio should be higher than 4. Based on the reported data in Table 2s, all models' adequate precision ratio is higher than 4, implying the provided models' high precision.

4.2. The effects of mill rotating speed and fractional mill filling

Fig. 4 illustrates the mutual effect of mill rotating speed and fractional mill filling on balls' dynamic voidage for all Bond's proposed BSDs. The dynamic voidage was found to increase with the mill rotating speed increase but decrease with increasing the fractional mill filling, as shown in Fig. 4. As depicted, the maximum value of dynamic voidage occurs in the maximum value of rotating speed and the minimum value of fractional mill filling for all BSDs. This is due to the influence mill rotating speed, and fractional mill filling have on the balls' motion. As the balls' motion is one of the layers sliding over one another, as the speed increases, the layers move faster with respect to one another, and the displacement amplitude between layers increases. In other words, they effectively "vibrate" more. Conversely, as the fractional mill filling (ball load) increases the ball layers' pressure increases and dampens the amplitude. Therefore, balls' layer arrangement relative to each other plays a vital role in the balls' voidage. For convenience, Fig. 5, which graphically presents four different non-random arrangements of mono-sized balls' layers, can well describe the effect of the arrangements of balls' layers on the voidage value. As can be seen, the loosest balls' arrangement is the cubic with a voidage of 47.64 % and the lowest number of spheres in contact, and the closest balls' arrangement is rhombohedral with a voidage of 25.95 %. It should be noted that the minimum voidage of mono-sized balls for a formed random balls' arrangement under vigorously shaking and vibrating is reported to equal to 35.9 % (Herdan, 1690; Yang, 2003).

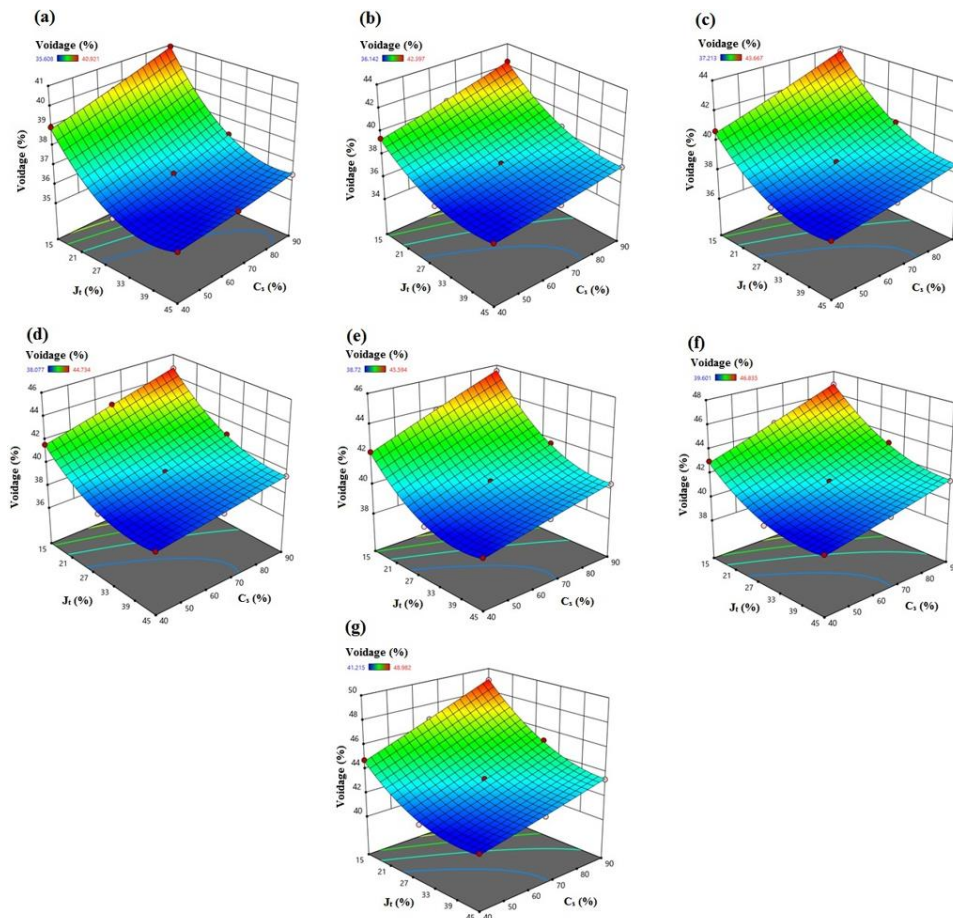


Fig. 4. The mutual effect of mill rotating speed and fractional mill filling on balls' voidage. (a) BSD₁; (b) BSD₂; (c) BSD₃; (d) BSD₄; (e) BSD₅; (f) BSD₆; (g) BSD₇

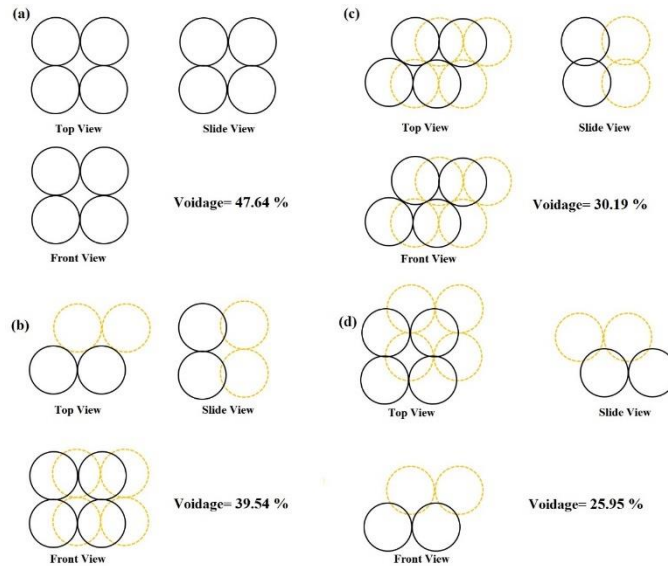


Fig. 5. Four arrangements of mono-sized balls. (a) Cubic, (b) Two orthorhombic, (c) One-tetragonal-spheroidal, (d) Two rhombohedral (Herdan, 1690; Yang, 2003)

4.3. Effect of ball size distribution

As mentioned above, the static voidage of Bond's proposed BSDs was also measured. Fig. 6 illustrates a comparison of the static voidage of BSDs. As depicted, the minimum and maximum static voidage occur for BSD₁ and BSD₇, respectively. Moreover, according to Table 2, for all values of C_s and J_t , the dynamic voidage is maximum in BSD₇ (in the range of 41.22 to 48.98 %) and minimum in BSD₁ (in the range of 35.61 to 40.92 %). Since the variation range of spherical particles' diameter has the most effect on the bed voidage, a statistical index representing the balls' dimensional dispersion must be chosen to analyze these results. To this end, the mean absolute deviation (MAD) of balls' diameter as a suitable measure of dispersion was selected. The MAD, a dimensionless statistical index, measures how much the values in a data set are likely to differ from their mean (Christine et al., 2007). Hence, the following Eq., which gives the MAD of balls' diameter, was employed:

$$\text{MAD} = \frac{\sum_{i=0}^n |D_i - D_m|}{n} \quad (15)$$

where D_i is the balls' diameter values in a given BSD (in millimeters), D_m is the balls' mean diameter (in millimeters), and n is the balls' number.

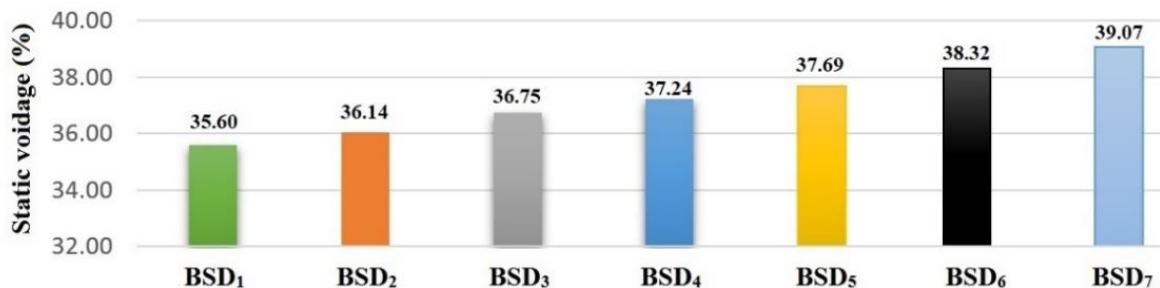


Fig. 6. Static voidage of proposed grinding media size distributions by Bond for the ball mills' first filling in commissioning

The MAD of the balls' diameter is reported in Table 4 for Bond's proposed BSDs. As can be seen, the maximum MAD is associated with the BSD₁, which has the minimum voidage. Moreover, its minimum occurs for the BSD₇, which has maximum voidage. These results show that the balls' voidage has a significant relationship with the dispersion of balls' diameter so that more MAD leads to decreasing the voidage and denser load because the smaller balls somehow fit into the gaps between the larger balls.

Likewise, others have reported similar results, indicating that the density of a multi-sized particle system increases with extending the particle size distribution resulting from more balls' dimensional dispersion (Sohn and Moreland, 1968; Bierwagen and Sanders, 1974; Desmond and Weeks, 2014).

Table 4. The calculated MAD of balls' diameter for Bond's proposed BSDs.

Parameter	BSD ₁	BSD ₂	BSD ₃	BSD ₄	BSD ₅	BSD ₆	BSD ₇
MAD	24.621	22.071	18.460	15.622	11.773	8.972	5.660

Figs. 7a, 7b, and 7c illustrate the percentage increase in grinding media's dynamic voidage compared to its static voidage by increasing the mill rotating speed for fractional mill fillings by 15 %, 30 %, and 45 %, respectively. As depicted, the maximum and minimum percentage increase in voidage occur for BSD₇ and BSD₁, respectively. It can be attributed to the trapping of the small balls between the balls' moving layer, which causes decreasing the amplitude of the displacement between layers.

By employing the conducted experiments (Table 2) and considering the obtained MAD for different BSDs (Table 4), we attempted to develop a comprehensive Eq. in addition to Eqs. 8 to 14, which can predict the dynamic voidage of balls for different BSDs based on calculating the MAD of balls' diameter. To this end, we developed the following quadratic Eq. by using the multiple regression analysis tools in Minitab software:

$$\Phi = 48.309 - 0.4511 J_t + 0.11010 C_s - 0.3459 MAD + 0.006095 J_t^2 + 0.00332 MAD^2 - 0.001102 J_t C_s + 0.000982 J_t MAD - 0.001763 C_s MAD \quad (16)$$

where Φ is the dynamic voidage (%), J_t is the fractional mill filling (%), C_s is the fractional speed (%), and MAD is the mean absolute deviation of balls' diameter. As can be observed, in addition to the defined factors in Eqs. 8 to 14 (J_t , C_s , J_t^2 , and $J_t C_s$), the MAD of balls' diameter, its quadratic term (MAD^2), the interaction of MAD and fraction mill filling ($J_t MAD$), and the interaction of rotating speed and MAD ($C_s MAD$) are significant in predicting dynamic voidage.

The statistical output of the Minitab software, which reports the p-value and R-square of the developed regression model, is shown in Fig. 8. The reported p-value, which is considerably lower than 0.05, proves the model's significance. Moreover, the adjusted R-squared of 99.21 % indicates that the

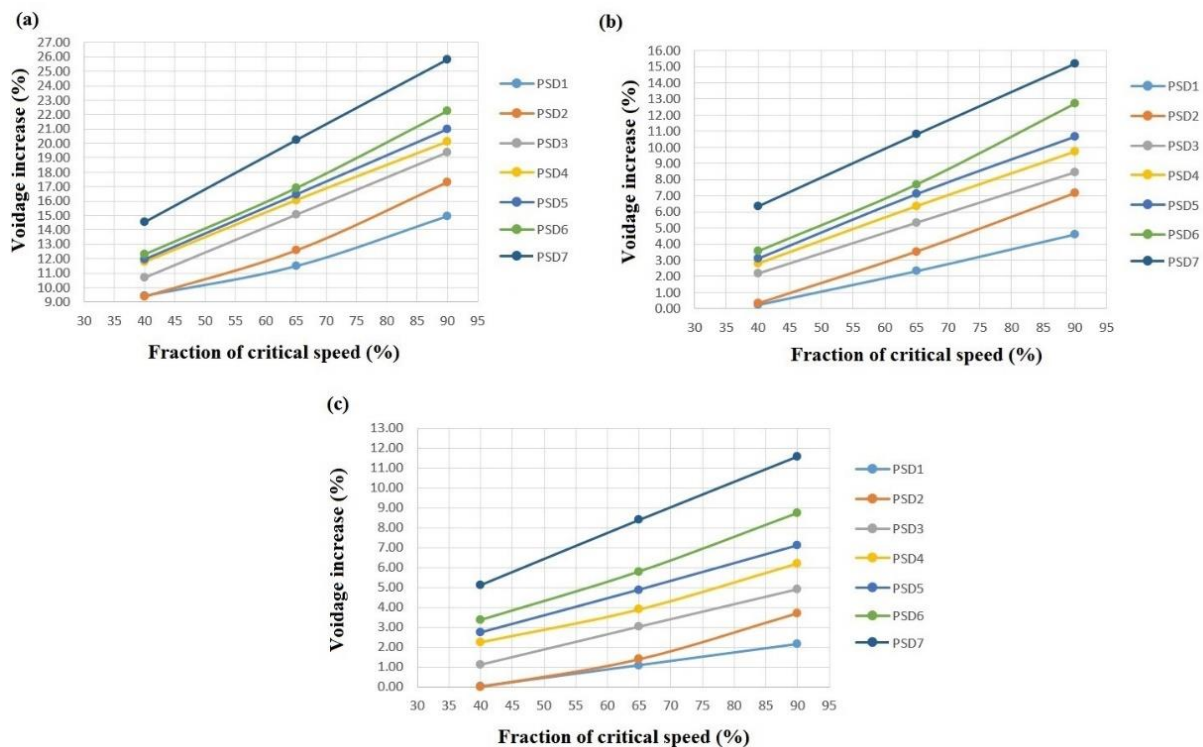


Fig. 7. The percentage increase in grinding media's dynamic voidage compared to its static voidage. (a) For $J_t=15$; (b) For $J_t=30$; (c) For $J_t=45$

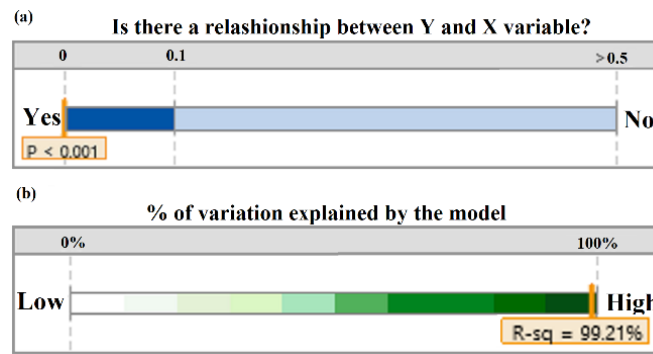


Fig. 8. The statistical output of the Minitab software. (a) P-value, (b) R-squared (R^2)

strength of the relationship between the model and the dependent variables is appropriate, leading to a good agreement between observed and predicted responses.

4.4. Models' validity and performances

Due to the almost broad ball size distribution inside the industrial ball mills, the first ball size distribution proposed by Bond (BSD_1), which includes balls with more diverse sizes, was selected as the closest BSD to actual industrial conditions to predict the voidage of grinding media inside the operational ball mills. For documenting this assumption, we cited the actual voidage of balls inside the 5 m diameter duty ball mill installed in the Sarcheshmeh copper complex processing plant (see Table 3s), measured by Hesami (2016). As shown in Table 3s, the static voidage for the balls inside the ball mill of the Sarcheshmeh site is reported to equal 36 %, close to obtained static voidage for BSD_1 (35.6 %). Fig. 9a shows the predicted dynamic balls' voidage through Eq. 8 associated with BSD_1 versus measured values. As illustrated, there is an acceptable and tangible agreement between predicted and actual data. Moreover, Fig. 9b shows an excellent predictive power of Eq. 16 in predicting the dynamic voidage of all Bond's proposed BSDs. From Fig. 9, Eqs. 8 and 16 can predict the grinding media's dynamic voidage with acceptable accuracy. Therefore, the charge's dynamic density can be obtained by replacing their output into Eq. 2 as the grinding media voidage value.

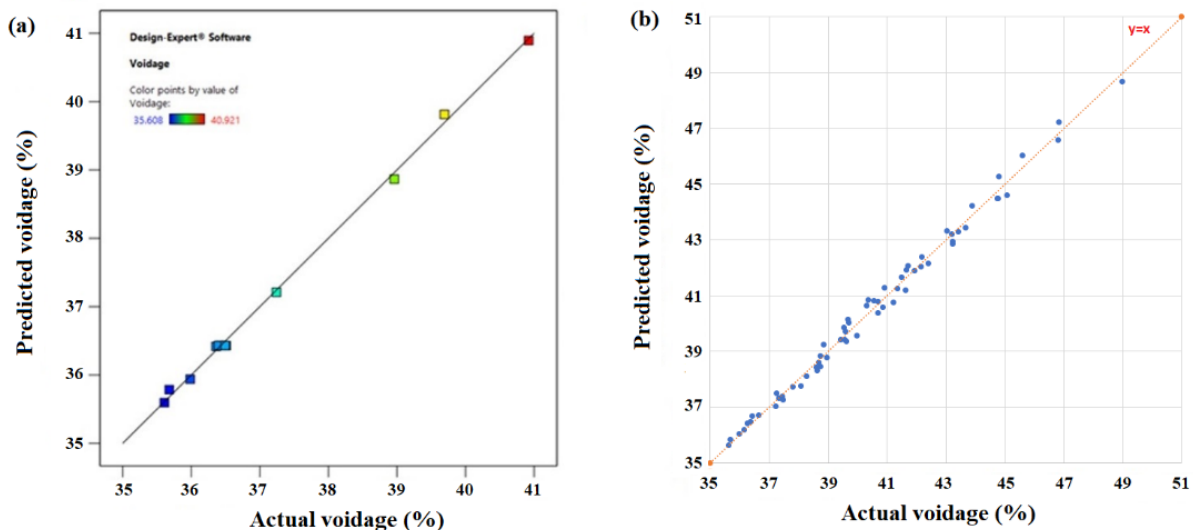


Fig. 9. Actual voidage vs. predicted by developed models. (a) Developed model for BSD_1 (Eq. 8), (b) Developed general multiple regression model for all BSDs (Eq. 16)

To assess the performance of Eqs. 8 and 16 to increase the Hogg and Fuerstenau model's accuracy, we applied the ball mills' database used by Morrell (1993) in his investigations (Table 5). It should be noted that we used MAD of 24.62 regarding BSD_1 to calculate the dynamic voidage through Eq. 16. Fig. 10 illustrates the predicted mills' power draw versus actual ones, respectively, for three separate cases: by supposing the grinding media voidage equal to 40% (Hogg and Fuerstenau's original model) and by

using Eqs. 8 and 16 to estimate balls' voidage (Modified versions of Hogg and Fuerstenau's model). Moreover, the actual power draw and predicted ones by the original and modified versions of the Hogg and Fuerstenau's model are reported in Table 5. The results imply that employing Eqs. 8 and 16 to estimate balls' voidage brings the predicted power closer to actual ones. Furthermore, the mean absolute percentage error (MAPE), an efficient method for measuring the prediction accuracy of models in statistics, was used to examine the effect of Eqs. 8 and 16 on the accuracy of Hogg and Fuerstenau's model. Low MAPE leads to higher predicting accuracy, so that MAPE less than 10 implies that the model has high predicting accuracy. The MAPE is defined as follows: (Kim and Kim, 2016):

$$\text{MAPE} = 100 \times \frac{1}{N} \sum_{t=1}^n \left| \frac{A_t - P_t}{A_t} \right| \quad (17)$$

where N is the number of data points, A_t is the actual value, and P_t is the predicted value.

The MAPE values are reported in Table 5. From Table 5, it is evident that the MAPE of Hogg and Fuerstenau's model is decreased by calculating grinding media voidage through Eqs. 8 and 16 by about 3.9 and 3.2 %, respectively. These results indicate a significant increase in the prediction accuracy of Hogg and Fuerstenau's model.

Table 5. Ball mill database (Morrell 1993), and the performance of original and modified versions of H&F model in predicting the industrial mills' power draw

Discharge mechanism	Diameter (m)	Length (m)	Fraction of Critical speed (%)	Ball fillin g (%)	Ore specific gravity (gr/cm ³)	Actual gross power (kW)	Predicted gross power (kW)			MAPE		
							Original H&F model	Modified H&F model (by using Eq. 8)	Modified H&F model (by using Eq. 16)	Original H&F model	Modified H&F model (by using Eq. 8)	Modified H&F model (by using Eq. 16)
Overflow	2.3	4.2	0.82	36	2.7	299	261.32	275.15	272.15	12.604	7.976	8.980
Overflow	2.65	3.4	0.77	36	2.7	334	301.43	317.39	313.93	9.751	4.972	6.010
Overflow	2.52	3.66	0.67	35	2.7	265	231.23	243.71	241.75	12.744	8.035	8.773
Overflow	3.48	4.62	0.71	39	2.7	834	719.92	759.93	753.59	13.679	8.881	9.642
Overflow	3.54	4.88	0.76	42	2.7	1029	864.88	912.67	904.62	15.949	11.305	12.087
Overflow	4.12	5.49	0.75	45	2.7	1600	1416.43	1492.92	1480.50	11.473	6.693	7.450
Overflow	4.38	7.45	0.75	30	2.7	2026	1951.32	2042.34	2021.04	3.686	0.806	0.220
Overflow	5.29	7.32	0.7	40	3.2	3828	3242.10	3420.28	3393.20	15.306	10.651	11.359
Overflow	4.8	6.1	0.69	40	3	2498	2084.84	2200.23	2183.11	16.540	11.920	12.606
Overflow	3.05	4.27	0.7	40	4.5	580	781.46	507.22	503.30	16.991	12.549	13.224
Overflow	2.6	3.7	0.69	40	4.5	347	275.91	290.69	288.50	20.488	16.227	16.859
Overflow	3.05	4.27	0.73	45	3.9	600	51.73	537.49	533.43	14.875	10.419	11.096
Overflow	3.5	4.42	0.74	35	2.75	820	701.53	738.71	731.75	14.447	9.913	10.762
Overflow	3.04	3.05	0.82	45	3.5	475	405.32	426.63	422.75	14.670	10.183	11.000
Overflow	2.29	2.74	0.83	44	3.5	235	163.26	171.93	170.30	30.526	26.839	27.531
Grate	1.7	2.7	0.81	40	2.7	103	80.62	85.05	84.19	21.732	17.432	18.263
Overflow	3.55	4.87	0.72	40	2.8	970	815.36	860.58	853.37	15.942	11.280	12.023
Overflow	3.5	4.75	0.75	42	2.8	921	808.37	852.94	845.59	12.229	7.390	8.188
Overflow	0.85	1.52	0.71	40	2.9	10	7.05	7.44	7.38	29.528	25.627	26.234
Overflow	0.85	1.52	0.71	20	2.9	6.8	4.83	4.94	4.90	28.954	27.294	28.000
Overflow	4.75	6.26	0.77	28	2.68	2050	1984.03	2068.72	2046.33	3.218	0.913	0.179
Overflow	3.85	5.9	0.77	30	2.8	1300	1150.51	1203.60	1190.86	11.499	7.415	8.396
Grate	2.64	3.66	0.7	43	2.8	420	288.43	304.32	302.02	31.326	27.542	28.091
Overflow	4.12	7.04	0.7	38	2.6	1800	1634.60	1725.44	1711.08	9.189	4.142	4.940
Overflow	3.48	6.33	0.75	34	2.7	1150	991.11	1042.65	1032.47	13.817	9.335	10.220

Overflow	5.34	8.69	0.73	28	3.2	3669	3517.01	3667.44	3631.67	4.143	0.043	1.017
Overflow	5.34	8.69	0.73	26	3.2	3549	3364.91	3494.97	3460.42	5.187	1.523	2.496
Overflow	5.34	8.69	0.73	24	3.2	3385	3197.57	3306.03	3272.99	5.537	2.333	3.309
Overflow	5.34	8.69	0.73	23	3.2	3251	3108.18	3205.54	3173.36	4.393	1.398	2.388
Overflow	5.33	8.54	0.72	34	2.6	4100	3722.35	3918.13	3882.19	9.211	4.436	5.312
Overflow	5.29	7.32	0.7	40	3.2	3828	3242.10	3420.28	3393.20	15.306	10.651	11.359
Overflow	4.87	8.84	0.75	30	2.6	3225	3014.83	3155.95	3123.72	6.517	2.141	3.140
Overflow	4.87	8.84	0.72	27	2.6	2900	2727.11	2841	2813.25	5.962	2.035	2.991
Overflow	4.85	5.92	0.73	41	2.9	2550	2207.78	2329.68	2310.14	13.420	8.640	9.406
Overflow	4.73	7.01	0.61	32	2.8	1840	1872.04	1968.69	1954.97	1.741	6.994	6.248
Overflow	4.68	5.64	0.72	48	2.8	2300	1925.51	2023.97	2009.72	16.282	12.001	12.621
Overflow	4.41	6.1	0.74	35	4.1	1900	1743.97	1833.35	1816.62	8.212	3.508	4.389
Overflow	4.1	5.92	0.75	34	3.1	1525	1402.16	1474.18	1459.96	8.055	3.333	4.265
Overflow	3.83	4.83	0.63	31	2.6	842	771.97	810.85	804.77	8.317	3.699	4.421
Overflow	2.6	4.57	0.75	34	2.65	400	345.04	363.02	359.47	13.739	9.246	10.133
The mean absolute percentage error (MAPE)										12.858	8.969	9.649

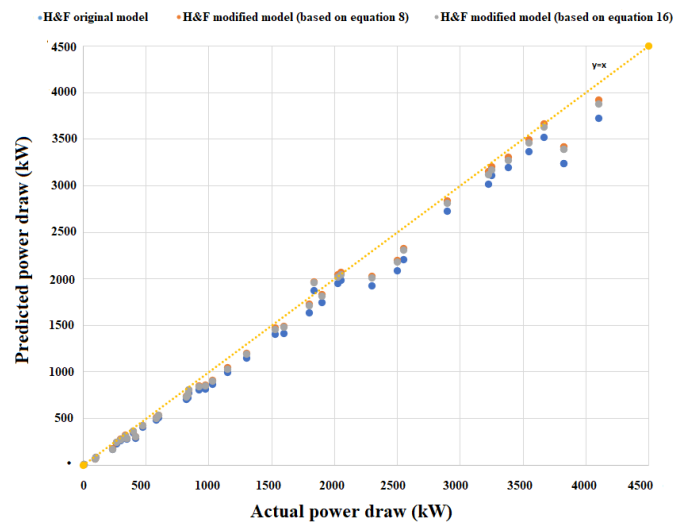


Fig. 10. Actual vs. predicted ball mills' power draw by original and modified versions of Hogg and Fuerstenau's model

5. Future Work

Although we have attempted to consider the effect of more critical milling parameters, including fractional mill filling, rotating speed, and grinding media size distribution on the grinding media voidage, we believe that there are still some gaps in our knowledge in this field. Since conducting experiments based on considering all possibilities is very time-consuming, examining the impact of some parameters on the voidage value has been left for the future due to lack of time. We believe that future studies should focus on the following items:

1. We think that the Liner/lifter geometry can have an effect on the media voidage by changing the balls' layers arrangement. Since the arrangement of balls' layers affects the voidage value (see Fig. 1), examining the impact of different liner geometries on the grinding media's voidage can be considered for future studies.
2. Although more than 90 % of whole mineral processing operations use balls as grinding media, other media shapes comprised of bars, cylpebs, ellipsoids, etc., are used in mineral processing plants (Aldrich, 2013; Shahbazi et al., 2020). According to the literature, particles' shape significantly affects the

Table 2s. Results of analysis of variance

BSDs	Source	Sum of squares	df	Mean Square	F-value	p-value (<i>prob</i> > <i>F</i>)	Adequate precision
BSD ₁	Model	32.92	5	6.58	852.41	< 0.0001	88.74
	J_t	22.50	1	22.50	2913.51	< 0.0001	
	C_s	3.05	1	3.05	394.53	< 0.0001	
	$J_t * C_s$	0.3636	1	0.3636	47.07	0.0002	
	J_t^2	5.77	1	5.77	747.12	< 0.0001	
BSD ₂	Model	38.91	5	7.78	865.87	< 0.0001	97.92
	J_t	25.05	1	25.05	2787.05	< 0.0001	
	C_s	7.39	1	7.39	822.70	< 0.0001	
	$J_t * C_s$	0.6642	1	0.6642	73.90	< 0.0001	
	J_t^2	4.72	1	4.72	525.45	< 0.0001	
BSD ₃	Model	41.30	5	8.26	488.53	< 0.0001	74.23
	J_t	26.66	1	26.66	1576.83	< 0.0001	
	C_s	8.22	1	8.22	486.31	< 0.0001	
	$J_t * C_s$	0.6440	1	0.6440	38.09	0.0005	
	J_t^2	4.66	1	4.66	275.87	< 0.0001	
BSD ₄	Model	45.16	5	9.03	1015.75	< 0.0001	106.32
	J_t	29.29	1	29.29	3294.46	< 0.0001	
	C_s	8.58	1	8.58	965.02	< 0.0001	
	$J_t * C_s$	0.6642	1	0.6642	74.71	< 0.0001	
	J_t^2	5.57	1	5.57	626.45	< 0.0001	
BSD ₅	Model	45.79	5	9.16	1277.05	< 0.0001	121.45
	J_t	28.42	1	28.42	3963.62	< 0.0001	
	C_s	10.41	1	10.41	1451.26	< 0.0001	
	$J_t * C_s$	0.7709	1	0.7709	107.50	< 0.0001	
	J_t^2	5.38	1	5.38	750.57	< 0.0001	
BSD ₆	Model	48.44	5	9.69	419.24	< 0.0001	71.74
	J_t	27.52	1	27.52	1190.82	< 0.0001	
	C_s	14.65	1	14.65	634.08	< 0.0001	
	$J_t * C_s$	0.7578	1	0.7578	32.79	0.0007	
	J_t^2	4.56	1	4.56	197.15	< 0.0001	
BSD ₇	Model	55.44	5	11.09	574.04	< 0.0001	84.46
	J_t	31.59	1	31.59	1635.50	< 0.0001	
	C_s	17.19	1	17.19	889.88	< 0.0001	
	$J_t * C_s$	1.01	1	1.01	52.29	0.0002	
	J_t^2	4.69	1	4.69	242.98	< 0.0001	

Table 3s. Size distribution and static voidage of balls inside the operational ball mill of the Sarcheshmeh copper complex processing plant (Hesami, 2016)

Ball size distribution							Static voidage (%)
Size (mm)	+70	-70+60	-60+50	-50+40	-40	Worn balls	36
Percentage weight	47.5	27.2	14.1	5.8	1.6	4	

References

- ALDRICH, C., 2013. *Consumption of steel grinding media in mills - A review*. Minerals Engineering, 49, 77-91.
- AMANNEJAD, M., BARANI, K., 2020. *Effects of ball size distribution and mill speed and their interactions on ball milling using DEM*. Mineral Processing and Extractive Metallurgy Review, 42, 1-6.
- Benyahia, F., O'Neill, K. E., 2005. *Enhanced Voidage Correlations for Packed Beds of Various Particle Shapes and Sizes*. Particulate Science and Technology, 23, 169-177.
- BIERWAGEN, G.P., SANDERS, T.E., 1974. *Studies of the Effects of Particle Size Distribution on the Packing Efficiency of Particles*. Powder Technology, 10, 111-119.
- BOND, F.C., 1958. *grinding ball size selection*. Trans AIME, 211, 592-595.
- CHRISTINE, F., KADER, G., MEWBORN, D., MORENO, J., Peck, R., Perry, M., Scheaffer, R., 2007. *Guidelines for Assessment and Instruction in Statistics Education*. Boston: American Statistical Association.
- CLEARY, P., AND OWEN, P., 2019, *effect of particle shape on structure of the charge and nature of energy utilization in a SAG mill*. Mineral engineering, 132, pp. 48-68.
- CORNEILLE, E. K., 1987. *Design, capital and operating costs of mineral processing plants*. Mineral Processing and Extractive Metallurgy Review, 4, 255-288.
- DAVIS, E.W, 1919. *Fine crushing in ball mills*. AIME Transactions, 61, 250 -296.
- DESMOND, K.W., WEEKS, E.R., 2014. *Influence of particle size distribution on random close packing of spheres*. Physical review Journal, 90, 022041-6.
- DJORDJEVIC, N., 2003. *Discrete element modelling of power draw of tumbling mills*. Mineral Processing and Extractive Metallurgy, 112, 109-114.
- DOLL, A. G., 2016. *An updated data set for sag mill power model calibration*. XXVIII International Mineral Process Congress, Quebec, Canada, 1-22.
- DRZYMALA, J., 2007. *Mineral processing: foundations of theory and practice of metallurgy*. Poland: Wroclaw University of Technology
- ERDEM, A. S., ERGUN, S. L., BENEZER, A. H., 2004. *Calculation of the power draw of dry multi-compartment ball mills*. Physicochemical Problems of Mineral Processing, 38, 221-230.
- FOSZCZ, D., WOŁOSIEWICZ-GLAB, M., KRAUZE, O., OGONOWSKI, S., GAWENDA, T., 2019. *Influence of grinding media movement on the throughput of dry grinding circuit with the electromagnetic mill*. MEC 2019, 1-6.
- GLENCORETECHNOLOGY. *IsaMill™ uses horizontal milling to secure better energy efficiency, product size and availability*. Available online: <https://www.glencoretechnology.com/en/technologies/isamill/> (accessed on 26 July 2022).
- GOLPAYEGANI, M., REZAI, B., 2022. *Modeling the power draw of tumbling mills: A comprehensive review*. Physicochem. Probl. Miner. Process., 58, 151600.
- GOLPAYEGANI, M.H., ABDOLLAHZADEH, A.A., 2017. *Optimization of operating parameters and kinetics for chloride leaching of lead from melting furnace slag*. Trans. Nonferrous Met. Soc. China, 27, 2704-2714.
- GÓRALCZYK, M., KROT, P., ZIMROZ, R., AND OGONOWSKI, S., 2020. *Increasing Energy Efficiency and Productivity of the Comminution Process in Tumbling Mills by Indirect Measurements of Internal Dynamics – An Overview*. energies, 13, 6735.
- GOVENDER, N., RAJ RAJAMANI, R. K., DANIEL N. WILKE, D. N., CHUAN-YU WU, C., JOHANNES KHINAST, J., GLASSER, B. J., 2018. *Effect of particle shape in grinding mills using a GPU based DEM code*. Minerals Engineering, 129, 71-84.
- GOVENDER, N., RAJAMANI, R. K., KOK, S., WILKE, D. N., 2015. *Discrete element simulation of mill charge in 3D using the BLAZE-DEM GPU framework*. Minerals Engineering, 79, 152-168.
- Gutiérrez, A., Ahues, D., González, F., Merino, P., 2019. *Simulation of Material Transport in a SAG Mill with Different Geometric Lifter and Pulp Lifter Attributes Using DEM*. Mining, Metallurgy & Exploration, 36, 431-440.
- Harris, J. W., Stocker, H., 1998. *Segment of a Circle*. In: *Handbook of Mathematics and Computational Science*. New York; Springer-Verlag.
- Herdan, G., 1960. *Small Particle Statistics*. 2nd ed, New York: Butterworth.
- Hesami, R., 2016. *A laboratory investigation of the effect of charge density on power draw in tumbling mills*. Master thesis. Bahonar University. (In Persian)
- Hilden, M. M., Powell M.S., Yahyaei, M., 2021. *an improved method for grinding mill filling measurement and the estimation of load volume and mass*. Minerals engineering, 160, 106638.

- HLOSTA, J., JEZERSKÁ, L., ROZBROJ, J., ŽUROVEC, D., NEČAS, J., ZEGZULKA, J., 2020. *DEM Investigation of the Influence of Particulate Properties and Operating Conditions on the Mixing Process in Rotary Drums: Part 1 – Determination of the DEM Parameters and Calibration*. Processes, 8, 1-26.
- HOGG, R., AND FUERSTENAU, D.W., 1972. *Power relationships for tumbling mills*. Trans. SME/AIME, 252, 418 - 423.
- KIANGI, K., POTAPOV, A., MOYS, M.H., 2013. *DEM validation of media shape effects on the load behaviour and power in a dry pilot mill*. Minerals Engineering, 46, 52-59.
- KIM, S., AND KIM, H. 2016. *A new metric of absolute percentage error for intermittent demand forecasts*. International Journal of Forecasting, 32, 669-679.
- KRAWCZYKOWSKI, D., FOSZCZ, D., OGONOWSKI, S., GAWENDA, T., WOŁOSIEWICZ-GLĄB, M., 2018. *Analysis of the working chamber size influences the effectiveness of grinding in the electromagnetic mill*. MEC 2018, 1-14.
- LATCHIREDDI, S.R., 2002. *modeling the performance of grates and pulp lifters in autogenous and Semiautogenous mills*. PhD thesis. University of Queensland.
- LI, T., S, LI., ZHAO, J., LU, P, MENG, L., 2012. *Sphericities of non-spherical objects*. Particuology, 10, 97-104.
- LIDDELL, K.S., MOYS, M.H., 1988. *the effects of mill speed and filling on the behaviour of the load in a rotary grinding mill*. Journal of South African Ins. Min. Metall., 88, 49 - 57.
- MISHRA, B.K., RAJAMANI, R.K., 1992. *the discrete element method for the simulation of ball mills*. Applied mathematical modeling, 16, 598-604.
- MOGROUP. *Metso Outotec Vertimill- Energy efficient gravity induced mill*. Available online: <https://www.mogroup.com/portfolio/vertimill/> (accessed on 26 July 2022).
- MOLYCOP, 2021, <https://molycop.com>.
- MONTGOMERY, D.C., 2005. *Design and Analysis of Experiments*. 6rd ed. New York: John Wiley and Sons.
- MORRELL, S., 1993. *the prediction of power draw in wet tumbling mills*. PhD thesis. University of Queensland.
- MORRELL, S., 2016. *modelling the influence on power draw of the slurry phase in Autogenous (AG), Semi-autogenous (SAG) and ball mills*. Minerals engineering, 89, 145-156.
- MORRELL, S., 2019. *Testing and calculations for Comminution machines*. in: Kumar Kavatra, S., Young, C.A., (Eds.), SME Mineral Processing & Extractive Metallurgy Handbook. Englewood: Society for Mining, Metallurgy, and Exploration (SME).
- MOYS, M.H., 1993. *A Model of mill power as affected by mill speed, load volume, and liner design*. The Southern African Institute of Mining and Metallurgy, 93, 135-141.
- PANJIPOUR, R., BARANI, K., 2014. *the effect of ball size distribution on power draw, charge motion and breakage mechanism of tumbling ball mill by discrete element method (DEM) simulation*. Physicochem. Probl. Miner. Process, 54, 258-269.
- RAJAMANI, R.K., KUMAR, P., GOVENDR, N., 2019. *The evaluation of grinding mill power models*. Mining, Metallurgy and Exploration, 36, 151-157.
- SHAHBAZI, B., JAFARI, M., PARIAN, M., ROSENKRANZ, J., CHEHREH CHELGANI, S., 2020. *Study on the impacts of media shapes on the performance of tumbling mills – A review*. Minerals Engineering, 157, 106490.
- SOHN, H. Y., MORELAND, C., 1968. *The effect of particle size distribution on packing density*. CJChE, 46, 162-167.
- SOLEYMANI YAZDI, M.R., KHORRAM, A., 2010. *Modeling and Optimization of Milling Process by using RSM and ANN Methods*. IJET, 2, 474-480.
- TAVARES, L., 2017. *A Review of Advanced Ball Mill Modeling*. Powder and particle, 34, pp. 106-124.
- U.S. DOE, 2007. *Mining industry energy bandwidth study*. Washington, United States: U.S. Department of Energy.
- VALERY, W., JANKOVIC, A., 2002. *the future of Comminution*. 34th International October Conference on Mining and Metallurgy, 287-298.
- VAN NIEROP, M.A., GLOVER, G., HINDE, A.L., MOYS, M.H, 2001. *A Discrete element method investigation of the charge motion and power draw of an experimental two-dimensional mill*. Int. J. Miner. Process, 61, 77-92.
- WHITE, H.A., 1905. *Theory of tube-mill action*. Jour. Chem. Met. and Min. Soc. of South Africa, 5, 290-305.
- WILLS, B. A., FINCH, J. A., 2016. *mineral processing technology: an introduction to the practical aspects of ore treatment and mineral recovery*. Amsterdam: Elsevier.
- WOŁOSIEWICZ-GLĄB, M., FOSZCZ, D., GAWENDA, T., SZYMON, O., 2016. *Design of an electromagnetic mill. Its technological and control system structures for dry milling*. MEC 2016, 1-6.

- WOŁOSIEWICZ-GŁAB, M., FOSZCZ, D., SARAMAK, D., GAWENDA, T., KRAWCZYKOWSKI, D., 2017. Analysis of a grinding efficiency in the electromagnetic mill for variable process and feed parameters. *MEC* 2017, 1-6.
- YANG, W. C., 2003. *Liquid-solids Fluidization*. in: Yang, W. C., (Ed.), *Handbook of Fluidization and Fluid-Particle System*. New York: Marcel Dekker.
- ZHANG, J., BAI, Y., DONG, H., WU, Q., YE, X., 2014. *Influence of ball size distribution on grinding effect in horizontal planetary ball mill*. *Advanced Powder Technology*, 25, 983-90.